JACS
JOURNAL OF THE AMERICAN CHEMICAL SOCIETY

Article

pubs.acs.org/JACS

Charge Photogeneration in Donor–Acceptor Conjugated Materials: Influence of Excess Excitation Energy and Chain Length

Raphael Tautz,[†] Enrico Da Como,[*,‡] Christian Wiebeler,[§] Giancarlo Soavi,[∥] Ines Dumsch,[⊥] Nils Fröhlich,[⊥] Giulia Grancini,[#] Sybille Allard,[⊥] Ullrich Scherf,[⊥] Giulio Cerullo,[∥] Stefan Schumacher,[§] and Jochen Feldmann[†]

[†]Photonics and Optoelectronics Group, Department of Physics and CeNS, Ludwig-Maximilians-Universität München, Amalienstr. 54, 80799 Munich, Germany

[‡]Department of Physics, University of Bath, Claverton Down, Bath BA2 7AY, United Kingdom

[§]Physics Department and Center for Optoelectronics and Photonics Paderborn (CeOPP), Universität Paderborn, Warburger Strasse 100, 33098 Paderborn, Germany

[∥]IFN-CNR, Dipartimento di Fisica, Politecnico di Milano, Piazza L. da Vinci 32, 20133 Milano, Italy

[⊥]Macromolecular Chemistry Group and Institute for Polymer Technology, Bergische Universität Wuppertal, Gaussstr. 20, 42119 Wuppertal, Germany

[#]Center for Nano Science and Technology@PoliMi, Istituto Italiano di Tecnologia, Via Giovanni Pascoli 70/3, 20133 Milano, Italy

Supporting Information

ABSTRACT: We investigate the role of excess excitation energy on the nature of photoexcitations in donor–acceptor π-conjugated materials. We compare the polymer poly(2,6-(4,4-bis(2-ethylhexyl)-4H-cyclopenta[1,2-*b*;3,4-*b′*]dithiophene)-4,7-benzo[2,1,3]thiadiazole) (PCPDTBT) and a short oligomer with identical constituents at different excitation wavelengths, from the near-infrared up to the ultraviolet spectral region. Ultrafast spectroscopic measurements clearly show an increased polaron pair yield for higher excess energies directly after photoexcitation when compared to the exciton population. This effect, already observable in the polymer, is even more pronounced for the shorter oligomer. Supported by quantum chemical simulations, we show that excitation in high-energy states generates electron and hole wave functions with reduced overlap, which likely act as precursors for the polaron pairs. Interestingly, in the oligomer we observe a lifetime of polaron pairs which is one order of magnitude longer. We suggest that this behavior results from the intermolecular nature of polaron pairs in oligomers. The study excludes the presence of carrier multiplication in these materials and highlights new aspects in the photophysics of donor–acceptor small molecules when compared to polymers. The former are identified as promising materials for efficient organic photovoltaics.

1. INTRODUCTION

The photogeneration of charge carriers in organic semiconducting materials remains a fascinating topic which involves several studies spanning more than two decades of research.[1−15] While being of fundamental relevance, it is also a topic of interest for the application of these materials in photovoltaics.[16−18] The general question of what are the primary photoexcitations in organic semiconductors cannot be answered without a detailed study of the molecular structure of the materials and the excess energy with which an excited state is generated.[19−21] Experiments on both disordered conjugated polymers and well-ordered small molecule single crystals have shown that a certain amount of charge carriers is generated upon photoexcitation.[22,23] However, how this occurs and to what extent is sometimes very difficult to address in a reliable and accurate way.

The initial picture that the primary photoexcitations in disordered conjugated polymers are free polarons has been disproved by a number of ultrafast spectroscopy experiments,[3,24] clearly pointing out that strongly bound Frenkel excitons are first generated as the majority of photoexcitations. Several experiments based on pump−probe spectroscopy in the visible, infrared, and terahertz spectral range have confirmed this picture.[8,25,26] In parallel with these studies there has been a growing interest in the detection and identification of loosely bound charge carrier pairs or polaron pairs.[6,27,28] These are believed to be the secondary species generated upon light absorption, since the low-dielectric constant of organic materials does not allow for charges to escape from the mutual Coulomb attraction even at room temperature.[29,30] The interest in polaron pairs recently has risen again, because of the application of conjugated polymers in bulk-heterojunction photovoltaics. Since polaron pairs exhibit a lower binding energy with respect to Frenkel excitons,[31] they might split into free polarons by exploiting heterojunctions with smaller energy offsets. This represents a substantial advantage in optimizing the available photovoltage in solar cells.[32]

Recently, a new class of π-conjugated semiconducting materials has been introduced exhibiting unique performances

Received: September 25, 2012
Published: February 25, 2013

dx.doi.org/10.1021/ja309252a | *J. Am. Chem. Soc.* 2013, 135, 4282−4290

in photovoltaic applications and in bipolar charge transport.[33−35] Their advantageous properties originate in the molecular structure, which can be tailored to provide the desired optoelectronic properties.[17,34,36] In these materials, two moieties with different electron affinity alternate along the molecular backbone, and the electronic coupling between them generates new electronic states, resulting in a narrow optical bandgap compared to widely used homopolymers and consequently better absorption in the red and near-infrared (NIR). Furthermore, our recent studies,[17] and from others,[37−39] showed that their chemical structure favors the formation of weakly bound polaron pairs, in absence of fullerenes or other electron-accepting compounds.

Two important classes of donor−acceptor copolymer have emerged with outstanding performances in photovoltaic blends: poly(thienothiophene benzodithiophene)[34] copolymers (PTB-type) and poly(cyclopentadithiophene benzothiadiazole)[40] copolymers (PCPDTBT-type). Ultrafast generation of polaron pairs has been reported for both systems, even in the absence of fullerene acceptors.[37,39] By performing a femtosecond absorption study in the infrared spectral range for a series of PCPDTBT copolymers, we have recently quantified the overall amount of polaron pairs formed from the initial photoexcitations.[17] Remarkably, this amount can be of the order of 24% and shows a strong dependence on the chemical structure of the polymer and the on-chain topology, i.e., the separation between the donor and acceptor moieties. These findings, together with the recent interest in donor−acceptor small-molecule-based organic photovoltaics,[41,42] prompted us to compare the photogeneration of charges in PCPDTBT and the respective oligomer.

Here, we present broadband femtosecond absorption spectroscopy of the polymer PCPDTBT and the oligomer CPDTBT. The broadband probe light allows us to monitor several excited species, excitons, and polaron pairs and to perform relative comparisons on their population. We address the role of photoexcitation excess energy in determining the nature of the primarily generated species, showing that a larger fraction results in polaron pairs as the excitation wavelength is tuned toward the blue part of the absorption spectrum. Supported by quantum chemical calculations, we show that excitation in high-energy states generates electron and hole wave functions with reduced overlap, which likely act as precursors for polaron pairs. Interestingly, we observe that the recombination lifetime of polaron pairs in the oligomer is 1 order of magnitude longer than the recombination lifetime in the polymer, suggesting that the oligomers and, in general, small-molecule donor−acceptor materials are systems capable of generating weakly bound long-lived polaron pairs that can be separated at suitable heterojunctions in solar cells.

2. EXPERIMENTAL AND COMPUTATIONAL METHODS

2.1. Material Synthesis. Reagents and dry solvents were purchased from Aldrich, ABCR Chemicals, or VWR International and were used without further purification. ^{1}H and ^{13}C NMR spectra were recorded on a Bruker Avance 400, chemical shifts are given in ppm. UV−vis and photoluminescence (PL) spectra were recorded with a Jasco V-670 and a Varian Cary Eclipse, respectively. Molecular weights of the polymer were determined by gel permeation chromatography analysis with polystyrene calibration. For mass spectrometry, a Fisons Instruments Sectorfield mass spectrometer VG instrument ZAB 2-SE-FDP at the MPI for Polymer Research (Mainz, Germany) was used.

PCPDTBT and CPDTBT are both generated in Stille-type cross-coupling reactions. The polymer PCPDTBT (M_n = 19 000 g/mol, M_w = 26 000 g/mol) was synthesized from 4,7-dibromobenzo[2,1,3]-thiadiazole and 2,6-bis(tributylstannyl)-4,4-bis(2-ethylhexyl)-4H-cyclopenta[2,1-*b*:3,4-*b*′]dithiophene according to a published procedure.[43] The PCPDTBT sample of this study shows long-wavelength absorption maxima at 730 and 747 nm in chloroform solution and as thin film, respectively; the solution emission maximum is observed at 786 nm (excitation wavelength 400 nm). The average number of repeat units in the polymer is 35 and 48 based on M_n and M_w estimations, respectively. 4-Bromo-7-methylbenzo[2,1,3]thiadiazole was prepared as described in literature.[44,45] The Stille-type cross coupling of 4-bromo-7-methylbenzo[2,1,3]thiadiazole (472 mg, 2.06 mmol) and 2,6-bis(tributylstannyl)-4,4-bis(2-ethylhexyl)-4H-cyclopenta[2,1-*b*:3,4-*b*′]dithiophene (1.01 g, 1.03 mmol) with Pd-$(PPh_3)_2Cl_2$ (11 mg, 15.45 μmol) as catalyst was carried out in dry toluene/THF (4/1, 50 mL) for 12 h under reflux. After purification (column chromatography, silica, *n*-hexane/toluene 1/1), the oligomer CPDTBT was obtained as a red solid. Yield: 703 mg (1.01 mmol, 98%). ^{1}H NMR ($C_2D_2Cl_4$, 400 MHz, 295 K): 0.58−0.65 (m, 12H), 0.88−1.07 (m, 18H), 1.94−2.04 (m, 4H), 2.72 (s, 6H), 7.34−7.38 (d, 7.4 Hz, 2H), 7.71−7.75 (m, 2H), 7.92−7.97 (m, 2H). ^{13}C NMR ($C_2D_2Cl_4$, 100 MHz, 295 K): 10.9, 14.3, 18.1, 23.0, 27.6, 28.6 34.4, 35.3, 43.0, 54.1, 122.2, 124.2, 126.1, 128.6, 129.5, 138.5, 139.8, 152.0, 156.0, 158.8. MS(FD) *m*/*z* = 698.3. UV−vis ($CHCl_3$): λ_{max} [nm] = 312, 371, 514. PL (λ_{ex} = 510 nm, $CHCl_3$): $\lambda_{em,max}$ [nm] = 658.

2.2. Sample Preparation. Pristine film samples of all studied materials were prepared from solution. The polymers and the oligomer have been dissolved in toluene (Chromasolv, Sigma-Aldrich) with concentrations of 10 and 20 mg/mL. To ensure good solubility, the solutions were stirred for several hours on a heating plate at 70 °C. The film samples have been prepared on microscope glass substrates by spin coating a volume of 80 μL at a speed of 1800 rpm for 2 min resulting in thin and homogeneous films with optical densities between 0.1 and 0.6 and a thickness between 50 and 150 nm. To prevent any oxidation or adsorption of water of the film samples, all steps were done in nitrogen atmosphere. Final encapsulation with thin microscope cover glass slides (about 100 μm thickness) using a vacuum glue (TORR SEAL, Thorlabs) allowed us to conduct our optical measurements in laboratory atmosphere without using vacuum to avoid photo-oxidation or other degradation phenomena.

Spectroscopy on chemically generated cations is described in details elsewhere.[17,46]

PL of all studied materials has been recorded with an automated UV−vis NIR PL spectrometer (Fluorolog, Horiba) using the same samples as measured in the ultrafast spectroscopic studies.

2.3. Ultrafast Spectroscopy. Time-resolved measurements were performed using a home-built femtosecond pump−probe setup. A Ti:sapphire regenerative amplifier (Quantronix, Integra C) was used as a laser source, delivering 100 fs pulses at a central wavelength of 800 nm with 1 mJ pulse energy at a repetition rate of 1 kHz. For the excitation pulses, a single-stage optical parametric amplifier (OPA), pumped at 400 nm, allowed the choice of a desired pump wavelength from 500 to 900 nm. UV wavelengths and wavelengths shorter than 500 nm were obtained by frequency doubling of the output of the OPA. Excitation pulse intensities were kept in the range between 5 and 50 $\mu J/cm^2$. In order to minimize bimolecular effects, the lowest possible excitation density has been chosen, which still provides a sufficient signal-to-noise ratio for clearly resolving the spectroscopic bands of all species. White light generated with a 2 and 3 mm-thick sapphire plate was used for probing in the visible from 450 to 780 nm and in the NIR from 820 to 1100 nm, respectively. For a spectrally resolved detection of the probe light, a spectrograph and CCD array (Stresing Entwicklungsbüro) were used.[47] The temporal chirp of the stretched white light pulse was carefully taken into account during the analysis and evaluation of the obtained two-dimensional (wavelength and time) $\Delta T(\lambda,t)/T$ maps before extraction of the spectral and temporal data with a homemade software. Overall, a temporal resolution of at least 150 fs was achieved for all excitation wavelengths.

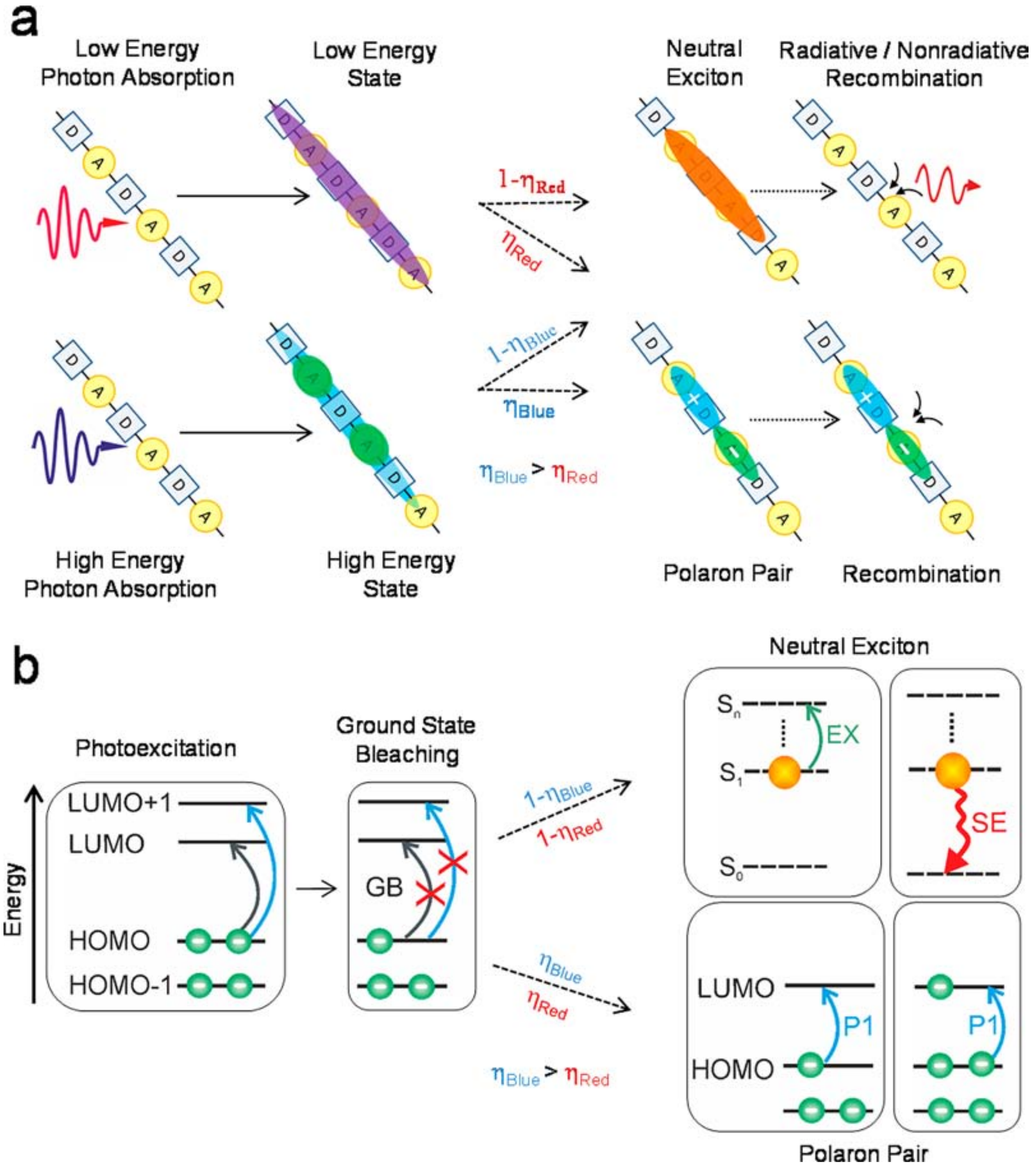

Figure 1. (a) Illustration of the photoinduced processes in donor−acceptor materials. Upon absorption of photons with high energy, states with more pronounced spatial separation of electron and hole wave functions are accessed. Upon relaxation from these excited states, pairs of charged polarons are formed with a yield η varying with excitation energy (η_{Red} and η_{Blue}) as well as neutral excitons with a yield $1 - \eta$. D and A denote donor and acceptor moieties in the molecular backbone. (b) Schematic visualization of the relevant energy levels for photoexcitation in a simplified single-particle picture. HOMO (LUMO) denotes the highest occupied (lowest unoccupied) molecular orbital and S_n marks exciton energy levels. Ground-state bleaching (GB) and the formed species, i.e., neutral excitons and polaron pairs, can be observed on an ultrafast time scale by their distinct spectroscopic signatures of excitonic absorption (EX), stimulated emission (SE), and polaronic absorption (P1), respectively.

2.4. Theoretical Methods. All calculations are based on density functional theory (DFT) and linear response time-dependent DFT (TD-DFT). The Gaussian09 program suite[48] was used, and all results presented were obtained with the Coulomb-attenuating method Becke three-parameter Lee−Yang−Parr hybrid functional (CAM-B3LYP) and 6-31G* basis set. Orbitals were visualized using GaussView 5 (ref 49). To model the PCPDTBT polymer as closely as possible, calculations were performed on a long but finite-length oligomer consisting of six units as shown in Figure 4; alkyl side chains that are largely uninvolved in the electronic processes studied here were replaced by methyl groups to reduce the computational cost. For CPDTBT, the calculations were done for the molecules used in the experiments including side chains. These have been removed from the visualizations in Figure 4 for clarity. For CPDTBT no symmetry constraints were imposed. Calculations for PCPDTBT were done for C_{2V} symmetry of the molecules, as previous tests show[46] that spectra and electronic states are very similar when considering a C_1 symmetry only. We first optimized the molecular geometry in the electronic ground state and then calculated the lowest electronic singlet excitations. A homogeneous broadening of 100 meV was applied to plot the electronic spectra. Natural transition orbitals (NTOs) were computed separately for the transitions of interest. In the donor−acceptor copolymers studied here, significant charge separation occurs in ground and excited states. To account also for long-range contributions to the electronic exchange interaction of these charges, we used the long-range corrected CAM-B3LYP functional.[46,50,51] Good convergence of the results was obtained with the 6-31G* basis set, which was used in all calculations presented here.

3. RESULTS AND DISCUSSION

3.1. Excess Energy Dependence of Polaron Pair Formation. In Figure 1 we provide a qualitative physical picture for the different steps in the photoinduced polaron pair

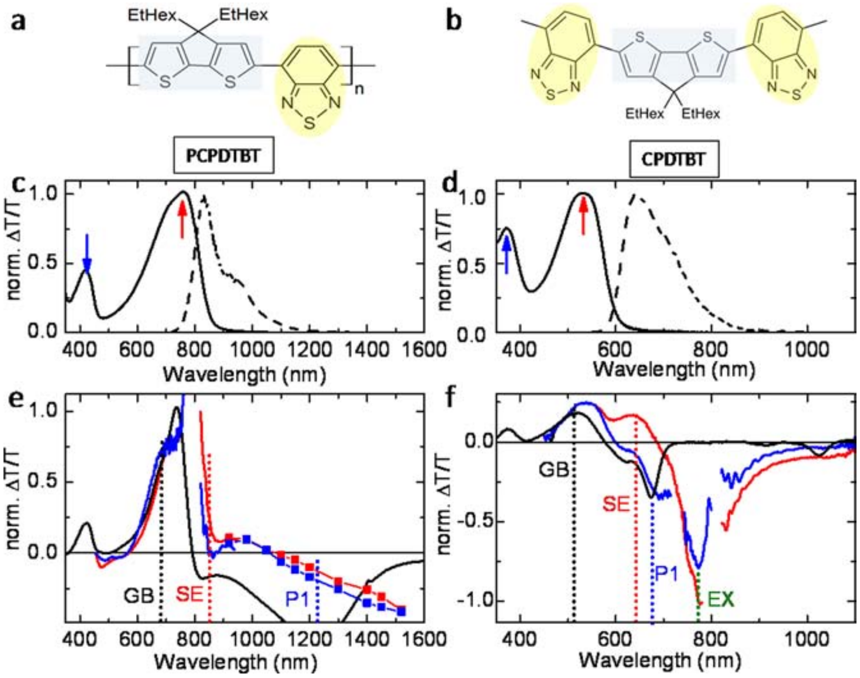

Figure 2. Chemical structures of (a) PCPDTBT and (b) CPDTBT. Gray- and yellow-shaded parts denote the donor and acceptor moieties, respectively. (c,d) Absorption (solid line) and PL (dashed line) spectra of thin film samples. Arrows indicate wavelengths for low- (red) and high-energy (blue) photoexcitation in pump−probe experiments. (e,f) Femtosecond transient absorption spectra for long- (red) and short-wavelength (blue) excitation compared with a spectrum of chemically generated cations (black). (e,f) Vertical dotted lines indicate the spectral position for the evaluation of the temporal dynamics of GB, EX, SE, and P1.

formation occurring at different excitation wavelengths. Figure 1a illustrates the formation of an excited state after photon absorption by the chromophore. Hereby, the energy of the absorbed photons, and hence the excess energy with respect to the gap, plays a crucial role for the degree of charge separation because of relaxation through the excited states. Higher photon energies excite the molecules to high electronic states. These may have a significantly more pronounced spatial separation of the pair of charge carriers (electron and hole) than states accessible at photon energies close to the optical bandgap,[52] as further explained below for our materials. In an intuitive picture, in high excited states a reduced overlap of the electron, and hole wave function is likely to be present causing a reduced Coulomb interaction. Thus, photoexcitations bearing significant excess energy should exhibit increased polaron pair formation yields η, i.e., the ratio of polaron pairs to neutral excitons photoinduced in the system.

Unique spectral signatures of excitons and polarons can be found in each material. A schematic visualization of corresponding energy levels and accessible transitions is presented in Figure 1b. The observation of ground-state bleaching (GB) is considered as a clear indication for the photoexcitation to higher electronic states of the molecules. Different species can be distinguished by their spectral signatures, giving rise to photoinduced absorption or stimulated emission (SE). Neutral excitons can be identified by stimulated emission or by their excited-state absorption band (EX). In contrast, the formation of polarons is visible from the characteristic polaronic absorption band (P1) below the optical bandgap of the neutral molecule.[17]

3.2. Spectroscopic Study of Polaron Pair Formation for Different Excess Energies.

In the following section, we discuss in detail our experimental and theoretical results, bearing in mind the qualitative picture we discussed in Figure 1. We have chosen a suitable set of materials, consisting of the copolymer PCPDTBT and the short oligomer CPDTBT. Their chemical structures are shown in Figure 2a,b, with the electron-donating cyclopentadithiophene moieties marked with a gray box and the accepting benzothiadiazole moieties highlighted with a yellow circle. Absorption and PL spectra of the respective materials are shown in Figure 2c,d. Pump−probe experiments with ≈100 fs time resolution and broadband-probe spectral range were performed on thin films of PCPDTBT and CPDTBT. Tuning of the pump wavelength allows us to excite the materials selectively in the low- and high-energy absorption bands, as indicated by red and blue arrows, respectively. In Figure 2e,f, differential transmission ($\Delta T/T$) spectra for low (red) and high (blue) excitation photon energies at 300 fs pump−probe delay are compared to a polaron absorption spectrum (black) obtained by chemical oxidation.[17,53] For better comparison, all spectra shown are normalized to their GB in a range separated from other spectral features and the pump laser wavelength. We have performed the normalization at 690 and 510 nm for the polymer and oligomer, respectively. In selecting these normalization wavelengths we have payed particular attention to maximize the overlap of the GB spectral shapes for the two excitation wavelengths, in a spectral range likely free from overlapping excited-state species, e.g., for the polymer 550−700 nm. In addition, this choice was operated after careful examination of the temporal dynamics of the GB spectra which we report in Figure S1. In particular at these normalization wavelengths, the $\Delta T/T$ spectra do not show appreciable spectral diffusion independently of the excitation wavelength and are therefore suitable to account for the density of photoexcitations induced in the sample by the pump.

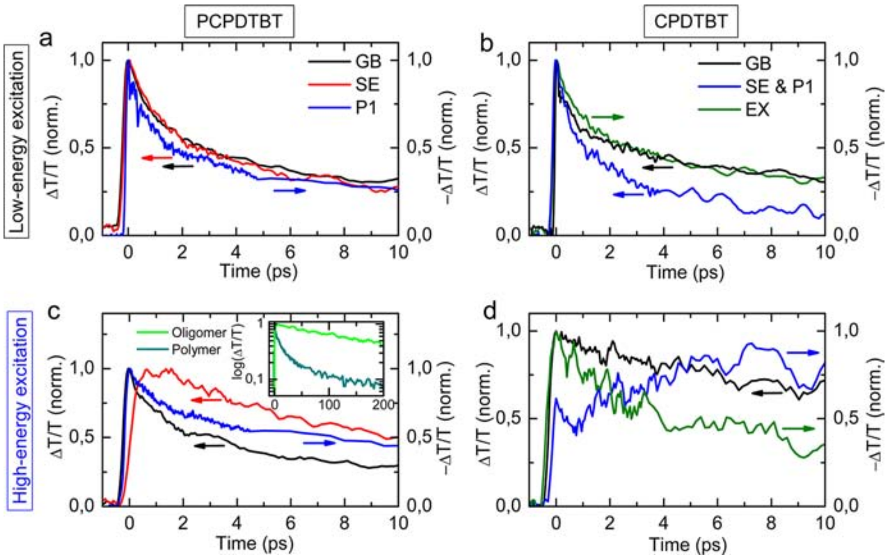

Figure 3. Ultrafast transient dynamics of GB (black), SE (red), P1 (blue), and EX (green) for long-wavelength excitation of (a) PCPDTBT (760 nm) and (b) CPDTBT (530 nm). (c,d) Dynamics for short-wavelength excitation at 400 and 370 nm are shown, respectively. For better comparison, the modulus of all normalized signals is plotted. Clear differences in the temporal dynamics between long- and short-wavelength excitation can be found for PCPDTBT in going from panels (a) to (c). Those are even more pronounced for the oligomer in panels (b) and (d). Spectral positions of respective probe wavelengths are indicated by vertical dotted lines in Figure 2e,f. The inset in panel (c) shows clearly longer decay dynamics for the polaron pair signal in the oligomer (light green) than in the polymer (dark green), both excited with excess energy.

For PCPDTBT in Figure 2e, both $\Delta T/T$ spectra upon 760 nm (red) and 400 nm (blue), as well as the chemical doping spectrum show a prominent GB from 570 up to 745 nm and a clear positive contribution peaking at 935 nm. Because of the good agreement with the spectral shape of the separately measured PL as shown in Figure 2c, an assignment of this latter contribution to stimulated emission is immediate. We note here that differences in the shape of the absorption spectrum and the GB are intrinsically connected to the dynamic nature of the GB. The GB spectrum measures the ground-state absorption blocking due to the population of excited states, which are no longer empty for an absorption process. The excited-state population evolves on a short time scale and involves potential energy surfaces which may be different from those probed in a linear absorption spectrum. At longer wavelengths up to 1100 nm the stimulated emission competes with the negative signal of the polaronic photoinduced absorption. Spectral features arising from polaron absorption range from ~800 nm and go up to 1400 nm, as seen in the spectrum of chemically generated cations; at 1100 nm polaron absorption becomes more prominent due to the vanishing stimulated emission, and the overall $\Delta T/\mathrm{T}$ curve turns negative. Our results demonstrate the presence of photogenerated polaron pairs for both excitation wavelengths with the polaron absorption bands exhibiting different amplitudes. When the excitation is performed at short wavelength (400 nm), a less-pronounced stimulated emission and enhanced polaronic absorption are an indication for a higher polaron-to-exciton ratio, i.e., $\eta_{\mathrm{Blue}} > \eta_{\mathrm{Red}}$.

When looking at the $\Delta T/T$ spectrum of the oligomer CPDTBT we observe a similar pattern of spectroscopic features (Figure 2f), but in addition it exhibits photoinduced absorption at 780 nm, which does not correspond to the PL or the radical cation (polaron) spectrum and occurs for both excitation wavelengths. For this material, the larger bandgap and thus blue-shifted absorption compared to the polymer allows to access the EX, which is located at lower energy compared to the polaron absorption, ranging between 700 and 1100 nm and peaking at 775 nm. As in the case of the polymer, excitation with high-energy photons with respect to the gap leads to a higher generation yield of polaron pairs. Because of the large overlap between SE and P1 in this material, the $\Delta T/T$ completely changes in the range around 630 nm. In agreement with our interpretation of a higher polaron pair generation yield when exciting at higher energy, the EX signal is reduced since its origin is excitonic.

The decay dynamics of all spectral features described in the polymer spectrum are shown in Figure 3a,c for 760 and 400 nm excitation, respectively. The polaron pair signal shows a rapid initial decay of 1.1 ps, followed by a slow decay with a time constant of 16 ps. Previous measurements of polaron pair dynamics, based on the decay of the mid-infrared absorption band P2 (ref 17), exhibit similar recombination dynamics with a first component lifetime of 2.6 ps and a second of 16 ps. Although we tried to stay at excitation densities as low as possible, the required densities for a broadband spectral detection of all species within one measurement did not allow us to completely suppress a residual contribution of bimolecular processes. Thus the discrepancy of the first component in the P1 lifetime with respect to the value in our previous experiments is likely due to the increased laser fluence resulting in an excitation density of 5×10^{18} cm^3, this is also likely the origin of the biexponential decay dynamics with 1.1 and 18 ps in the stimulated emission. The increased laser fluence compared to our previous experiments (excitation density 7×10^{17} cm^3) may have an effect on the generation of polaron pairs, since in some materials it has been reported that high excitation densities promote polaron pair formation. We have investigated this effect for our polymers and found that the $\Delta T/T$ signal amplitude for P1 and the first time constant shows a weak dependence on laser fluence, whereas the SE and GB signals are more affected (Figure S2). Therefore, we exclude that the higher excitation densities used in the experiments presented here have a significant influence on the polaron pair generation yield.

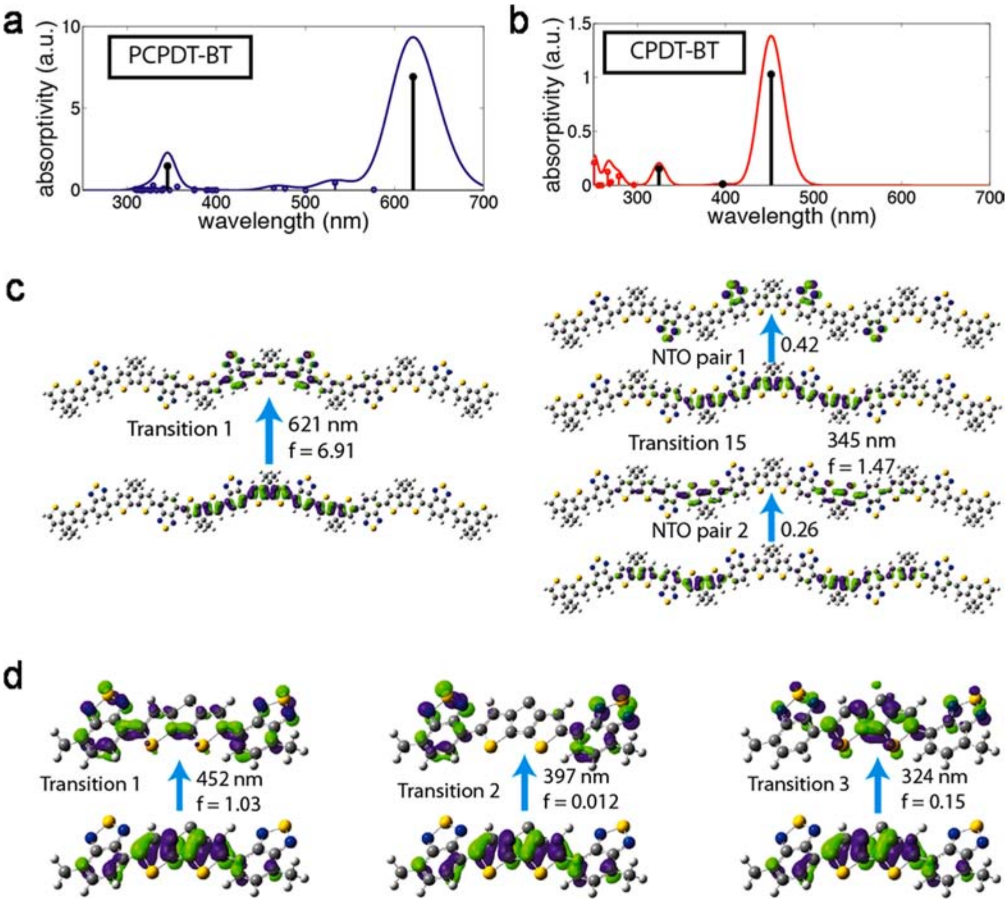

Figure 4. Calculated absorption spectra (a) and (b) and analysis of excitations in terms of natural transition orbitals (NTOs) for the copolymer PCPDTBT (c) and the oligomer CPDTBT (d). Stick spectra represent wavelength and oscillator strength of each transition in (a) and (b); those transitions used for the NTO analysis are shown in black. For both copolymer in (a) and oligomer in (b), only one transition with large oscillator strength contributes to the long-wavelength absorption peak. The corresponding pairs of NTOs are depicted in panels (c) and (d), respectively, showing a delocalized nature and direct spatial overlap of the wave functions. In contrast, transitions corresponding to the absorption band at shorter wavelength exhibit a much lower oscillator strength (denoted as *f*).

The GB has contributions from both polaron pairs and excitons since it measures the depletion of the ground-state absorption with no distinction on whether this originates from neutral or charged excited species. Interestingly, it has very similar decay dynamics to the stimulated emission and confirms the fact that excitons are formed predominantly when the polymer is excited at 760 nm. At short wavelength excitation, the fast initial decay component of the polaron pair signal is less pronounced, as shown in Figure 3c. In this case, the GB decays with a fast time constant of 1.2 ps and a second longer decay of 16 ps. These dynamics are comparable to that of polaron pair absorption, which show a biexponential decay with 1.6 and 17 ps time constants. While the values of the decay times are not identical overall, this suggests that a larger contribution of polaron pairs to the bleaching signal is present. In agreement with other studies,[51] a slower rise time can be observed for stimulated emission due to vibrational relaxation of the hot excited state preceding photon emission. Measurements on another donor−acceptor copolymers with a similar chemical structure (Figure S3) show qualitatively the same effect of a decreasing stimulated emission and increasing polaronic absorption for larger excess excitation photon energies. Excitation energies exceeding the optical bandgap twice did not show any indication of multiexciton or multipolaron pair formation, as known for other organic materials like pentacene[54−56] or carbon nanotubes.[57] This result confirms what has been recently observed by Bange et al. on ladder-type polymers.[58]

The temporal dynamics for the oligomer is shown in Figure 3b,d and confirms the hypothesis that excitation at higher energy leads to a more pronounced formation of polaron pairs. While in the long-wavelength excitation case the GB decay follows almost exactly the dynamics of the EX band (Figure 3b), it appears to be clearly slower when excited at higher energy (Figure 3d) and more similar to the P1 dynamics. We believe that a larger contribution of longer living polaron pairs is the reason for this prominent difference. When excited at 530 nm, the temporal dynamics of the spectral region from 600 to about 700 nm, where SE and P1 absorption are overlapping, is clearly dominated by SE. Although originating from the same species, i.e. excitons, the SE shows faster decay dynamics compared to EX. Most likely this occurs due to a spectrally overlapping polaron absorption signal. However, the most interesting results are obtained when molecules are excited at 370 nm. Here, a long-lived signal with negative amplitude due to polaron absorption follows the GB dynamics and, according to our assignment, is another strong indication that polaron pairs are the mainly formed species. What seems to be a slow buildup of polaron pair absorption can be explained as decay of SE having opposite sign. Indeed measurements of the P1 dynamics further into the red part of the spectrum at 700 nm instead of 640 nm (as in Figure 3d) do not exhibit such a rise on a picosecond time scale (Figure S4).

In summary, the materials show a higher polaron pair yield η for excitation with higher photon energies compared to excitations close to the optical bandgap, i.e., $\eta_{\mathrm{Blue}} > \eta_{\mathrm{Red}}$. This effect is present for the donor−acceptor copolymer PCPDTBT (and a similar polymer reported in Figure.S3) and is found to be significantly pronounced for the shorter oligomer CPDTBT. Interestingly, as shown in the inset in Figure 3c, the lifetime of the polaron pairs excited at high energy in the oligomer is 164 ps, an order of magnitude larger than the long component in the lifetime of the same species in the polymer, which is 16 ps.

3.3. Wave Function Localization of Photoexcited States. To obtain a deeper understanding and provide a more comprehensive explanation on the photon energy dependence of the polaron pair generation process, we investigated by quantum chemical modeling the optical transitions in PCPDTBT and CPDTBT (see Experimental and Computational Methods section for details). Figure 4a,b shows calculated linear absorption spectra. Comparing these computed spectra with experimental absorption spectra in Figure 2c,d, we note a consistent overall shift of calculated transitions to shorter wavelengths. More importantly, however, relative positions of transitions in the spectrum and relative oscillator strengths of the different peaks are well represented by the calculations. Figure 4c,d provides NTOs for the relevant optical transitions in PCPDTBT and CPDTBT. In the case of the polymer, excitation with low photon energy results in a transition (Figure 4c, transition 1) where both electron and hole wave function are delocalized over several benzothiadiazole (BT) and dithiophene units in the center of the chromophore. The resulting large wave function overlap and the common center of mass lead to a strong Coulomb interaction and explain the favored formation of neutral excitons with respect to spatially separated polaron pairs. The wave function distribution appears different, when electron and hole are excited with significant excess energy, as shown by the dominant NTO pairs 1 and 2 of transition 15 in Figure 4c (CI coefficients 0.42 and 0.26). This transition carries the main oscillator strength leading to the high-energy absorption band in the polymer, and the corresponding dominant NTOs clearly show its significant charge-transfer character. In the dominant contributions, the electron wave function is mostly localized on the BT units, whereas the hole wave function is delocalized in nature. The resulting spatial separation of electron and hole wave function leads to a reduced Coulomb interaction and consequently favors the formation of a weakly bound polaron pair. We note that we have found almost identical NTOs to those reported in Figure 4 for transitions calculated in the equilibrium geometries of the corresponding excited states.

An even more pronounced difference can be found for CPDTBT, as shown in panel Figure 4d. The long wavelength arises from a transition that is delocalized over the entire oligomer backbone. Both electron and hole wave functions are calculated to be spread out with their center of mass located in the middle of the molecule. Transition 3 in Figure 4d is responsible for the higher-energy absorption band in the oligomer and is accessible at high photon energy. This transition also appears to be very delocalized in nature with significant spatial overlap of electron and hole wave functions. However, following excitation of this transition, we assume that the system undergoes ultrafast relaxation through the manifold of excited states.[51] During this relaxation the system may transit through another excited state which is optically almost dark but has very pronounced *charge-transfer character* according to the involved NTOs shown in Figure 4d. In this state, the overlap between electron and hole wave functions is strongly reduced which could be the explanation for the increased polaron formation yield found at higher excitation energies for this system. The pronounced *charge-transfer character* of the excited states at higher energies explains also the lower oscillator strength for those transitions with a lower wave function overlap of initial and final state.[59] This can be seen in the measured (Figure 2c,d) and calculated (Figure 4a,b) absorption spectra showing lower absorption in the high-energy peaks. The corresponding oscillator strengths for the relevant transitions are given in Figure 4c,d.

We assume that topological restrictions due to a limited chain length of the oligomer further promote the localization of the electron wave function. This together with the longer lifetime of the polaron pairs in the oligomer clearly points toward dynamics involving intermolecular processes. In the oligomeric sample, it is likely that a close spacing between donor and acceptor units belonging to nearest-neighbor molecules is present in three dimensions. In case of favorable packing and orientation, this may favor the formation of stabilized long-lived polaron pairs, as was observed in copolymer heterojunctions.[60] While these aspects are important in trying to establish a quantitative comparison between the polymer and the oligomer, the experimental evidence for a higher polaron pair yield upon excitation with high photon energy can be rationalized by the intramolecular wave function characteristics shown in Figure 4. Simulations involving intermolecular polaronic states, for example in dimers, are likely to provide more information on the dynamics of polarons in both systems but involve a large number of degrees of freedom connected to the crystallinity and, in general, to the structure of the two materials. Such studies will be reported elsewhere. PCPDTBT is a semicrystalline polymer,[61] and we have indications that CPDTBT forms polycrystalline films, thus the two material systems have structural similarities. CPDTBT is a rather new compound, and a full structural characterization has not been carried out. Certainly molecular packing and crystallinity may be involved in the polaron pair recombination process, less likely in the generation which starts from the intramolecular wave function shown in Figure 4, since those are mainly responsible for light absorption.

4. CONCLUSIONS

In conclusion, we have studied the influence of excess excitation energy on charge photogeneration in organic donor−acceptor materials with different chain length. Both materials studied, i.e., PCPDTBT and CPDTBT, show consistently higher polaron pair yields for shorter excitation wavelengths together with a reduced occurrence of stimulated emission. With broadband ultrafast pump−probe spectroscopy, we demonstrated a significantly higher polaron-to-exciton formation ratio η for high-energy photons already within the temporal resolution of the setup of 150 fs ($\eta_{\mathrm{Blue}} > \eta_{\mathrm{Red}}$). This effect is observable in PCPDTBT and more pronounced for a short oligomer with the same chemical structure, CPDTBT.

We explain the higher polaron pair formation yield η observed at shorter wavelengths with the more pronounced initial charge-transfer character of the higher-lying excited states absorbing light, likely caused by the variation of the molecular on-chain energy landscape present in these materials. This interpretation is supported by our quantum chemical calculations. During the relaxation through the excited states in the oligomer CPDTBT, pronounced localization of the electron at the BT acceptor moieties occurs when excited at 370 nm. In contrast, the excitations stay delocalized over the entire molecule for 530 nm excitation. A similar effect occurs in PCPDTBT, although less pronounced. The reduced overlap between electron and hole leads to a decreased Coulomb attraction and a lower binding energy. We therefore conclude that a more pronounced charge separation in the initial excitations dynamically favors polaron pair formation instead of relaxation into a strongly bound and emissive Frenkel exciton.

The finding of a high polaron pair formation yield over the high energy part of the absorption spectrum indicates that an optimization of materials in terms of higher yields might be interesting for more efficient organic solar cells. Due to a lower binding energy, the extraction of polaron pairs might be favorable in terms of a reduced voltage loss for their separation compared to strongly bound Frenkel excitons. We believe that the knowledge gained about the nature of higher photoexcitations and the influence of the molecular size is crucial for reaching this goal. Interestingly, we report an increase by 1 order of magnitude in the lifetime of polaron pairs in the oligomer, which can represent an intrinsic advantage for organic photovoltaics. The increased lifetime may be related to a different crystalline, solid-state packing of the small molecules if compared to the semicrystalline polymer PCPDTBT; further detailed structural investigations are required to address this important difference.

■ ASSOCIATED CONTENT

S Supporting Information

Transient absorption spectra at several pump−probe delay times, transients at different excitation fluencies, photophysics of polymer PCPDT2TBT, SE transients of CPDTBT. This material is available free of charge via the Internet at http://pubs.acs.org.

■ AUTHOR INFORMATION

Corresponding Author

edc25@bath.ac.uk

Notes

The authors declare no competing financial interest.

■ ACKNOWLEDGMENTS

Financial support by the DFG for funding through the SPP1355 “Fundamental processes in organic photovoltaics” and the Nanosystems Initiative Munich (NIM) as well as by the Bavarian Ministry for Science through the initiative “Solar Technologies Go Hybrid” (SolTech) is gratefully acknowledged. R.T., E.D.C., G.S., and G.C. are grateful for the financial support by the European Community Access to Research Infrastructure Action, contract RII3-CT-2003-506350 (Centre for Ultrafast Science and Biomedical Optics, LASERLAB-EUROPE). G.C. acknowledges partial support by the PRIN Project 2008 JKBBK4 “Tracking ultrafast photoinduced intra- and intermolecular processes in natural and artificial photosensors”. The Paderborn group acknowledges financial support from the DFG (GRK 1464) and a grant for computing time at PC^2 Paderborn Center for Parallel Computing. We are grateful for open discussions with L. Luer, D. Polli, and M. T. Carlson.

■ REFERENCES

(1) Vardeny, Z.; Ehrenfreund, E.; Brafman, O.; Nowak, M.; Schaffer, H.; Heeger, A. J.; Wudl, F. *Phys. Rev. Lett.* **1986**, *56*, 671−674.

(2) Kersting, R.; Lemmer, U.; Mahrt, R. F.; Leo, K.; Kurz, H.; Bässler, H.; Göbel, E. O. *Phys. Rev. Lett.* **1993**, *70*, 3820−3823.

(3) Kersting, R.; Lemmer, U.; Deussen, M.; Bakker, H. J.; Mahrt, R. F.; Kurz, H.; Arkhipov, V. I.; Bässler, H.; Göbel, E. O. *Phys. Rev. Lett.* **1994**, *73*, 1440−1443.

(4) Barth, S.; Bässler, H. *Phys. Rev. Lett.* **1997**, *79*, 4445−4448.

(5) Hoofman, R.; de Haas, M. P.; Siebbeles, L. D. A.; Warman, J. M. *Nature* **1998**, *392*, 54−56.

(6) Schweitzer, B.; Arkhipov, V. I.; Bässler, H. *Chem. Phys. Lett.* **1999**, *304*, 365−370.

(7) Miranda, P. B.; Moses, D.; Heeger, A. J. *Phys. Rev. B* **2001**, *64*, 4.

(8) Hendry, E.; Schins, J. M.; Candeias, L. P.; Siebbeles, L. D. A.; Bonn, M. *Phys. Rev. Lett.* **2004**, *92*, 196601.

(9) Bässler, H. *Nat. Phys.* **2006**, *2*, 15−16.

(10) Virgili, T.; Marinotto, D.; Manzoni, C.; Cerullo, G.; Lanzani, G. *Phys. Rev. Lett.* **2005**, *94*, 117402.

(11) Scheblykin, I. G.; Yartsev, A.; Pullerits, T.; Gulbinas, V.; Sundström, V. *J. Phys. Chem. B* **2007**, *111*, 6303−6321.

(12) Banerji, N.; Cowan, S.; Leclerc, M.; Vauthey, E.; Heeger, A. J. *J. Am. Chem. Soc.* **2010**, *132*, 17459−17470.

(13) Deschler, F.; Da Como, E.; Limmer, T.; Tautz, R.; Godde, T.; Bayer, M.; von Hauff, E.; Yilmaz, S.; Allard, S.; Scherf, U.; Feldmann, J. *Phys. Rev. Lett.* **2011**, *107*, 127402.

(14) Grancini, G.; Martino, N.; Antognazza, M. R.; Celebrano, M.; Egelhaaf, H. J.; Lanzani, G. *J. Phys. Chem. C* **2012**, *116*, 9838−9844.

(15) Etzold, F.; Howard, I. A.; Forler, N.; Cho, D. M.; Meister, M.; Mangold, H.; Shu, J.; Hansen, M. R.; Mullen, K.; Laquai, F. *J. Am. Chem. Soc.* **2012**, *134*, 10569−10583.

(16) Sheng, C. X.; Tong, M.; Singh, S.; Vardeny, Z. V. *Phys. Rev. B* **2007**, *75*, 085206.

(17) Tautz, R.; Da Como, E.; Limmer, T.; Feldmann, J.; Egelhaaf, H.-J.; von Hauff, E.; Lemaur, V.; Beljonne, D.; Yilmaz, S.; Dumsch, I.; Allard, S.; Scherf, U. *Nat. Commun.* **2012**, *3*, 970.

(18) Rolczynski, B. S.; Szarko, J. M.; Son, H. J.; Liang, Y. Y.; Yu, L. P.; Chen, L. X. *J. Am. Chem. Soc.* **2012**, *134*, 4142−4152.

(19) Arkhipov, V. I.; Emelianova, E. V.; Bassler, H. *Phys. Rev. Lett.* **1999**, *82*, 1321−1324.

(20) Gadermaier, C.; Cerullo, G.; Sansone, G.; Leising, G.; Scherf, U.; Lanzani, G. *Phys. Rev. Lett.* **2002**, *89*, 4.

(21) Gao, J.; Hegmann, F. A. *Appl. Phys. Lett.* **2008**, *93*, 3.

(22) Hegmann, F. A.; Tykwinski, R. R.; Lui, K. P. H.; Bullock, J. E.; Anthony, J. E. *Phys. Rev. Lett.* **2002**, *89*, 4.

(23) Paquin, F.; Latini, G.; Sakowicz, M.; Karsenti, P. L.; Wang, L. J.; Beljonne, D.; Stingelin, N.; Silva, C. *Phys. Rev. Lett.* **2011**, *106*, 197401.

(24) Brabec, C. J.; Zerza, G.; Cerullo, G.; De Silvestri, S.; Luzzati, S.; Hummelen, J. C.; Sariciftci, S. *Chem. Phys. Lett.* **2001**, *340*, 232−236.

(25) Aryanpour, K.; Sheng, C. X.; Olejnik, E.; Pandit, B.; Psiachos, D.; Mazumdar, S.; Vardeny, Z. V. *Phys. Rev. B* **2011**, *83*, 5.

(26) Herrmann, D.; Niesar, S.; Scharsich, C.; Kohler, A.; Stutzmann, M.; Riedle, E. *J. Am. Chem. Soc.* **2011**, *133*, 18220−18233.

(27) Yan, M.; Rothberg, L. J.; Papadimitrakopoulos, F.; Galvin, M. E.; Miller, T. M. *Phys. Rev. Lett.* **1994**, *72*, 1104−1107.

(28) Mizes, H. A.; Conwell, E. M. *Phys. Rev. B* **1994**, *50*, 11243−11246.

(29) Hertel, D.; Bässler, H. *ChemPhysChem* **2008**, *9*, 666−688.

(30) Wang, Z. D.; Mazumdar, S.; Shukla, A. *Phys. Rev. B* **2008**, *78*, 235109.

(31) Hallermann, M.; Haneder, S.; Da Como, E. *Appl. Phys. Lett.* **2008**, *93*, 053307.

(32) Gong, X.; Tong, M. H.; Brunetti, F. G.; Seo, J.; Sun, Y. M.; Moses, D.; Wudl, F.; Heeger, A. J. *Adv. Mater.* **2011**, *23*, 2272−2277.

(33) Beaujuge, P. M.; Tsao, H. N.; Hansen, M. R.; Amb, C. M.; Risko, C.; Subbiah, J.; Choudhury, K. R.; Mavrinskiy, A.; Pisula, W.; Bredas, J. L.; So, F.; Mullen, K.; Reynods, J. R. *J. Am. Chem. Soc.* **2012**, *134*, 8944−8957.

(34) Chen, H. Y.; Hou, J. H.; Zhang, S. Q.; Liang, Y. Y.; Yang, G. W.; Yang, Y.; Yu, L. P.; Wu, Y.; Li, G. *Nat. Photonics* **2009**, *3*, 649−653.
(35) Svensson, M.; Zhang, F. L.; Veenstra, S. C.; Verhees, W. J. H.; Hummelen, J. C.; Kroon, J. M.; Inganas, O.; Andersson, M. R. *Adv. Mater.* **2003**, *15*, 988−991.
(36) Boudreault, P. L. T.; Najari, A.; Leclerc, M. *Chem. Mater.* **2011**, *23*, 456−469.
(37) Carsten, B.; Szarko, J. M.; Son, H. J.; Wang, W.; Lu, L. Y.; He, F.; Rolczynski, B. S.; Lou, S. J.; Chen, L. X.; Yu, L. P. *J. Am. Chem. Soc.* **2011**, *133*, 20468−20475.
(38) De, S.; Pascher, T.; Maiti, M.; Jespersen, K. G.; Kesti, T.; Zhang, F. L.; Inganas, O.; Yartsev, A.; Sundstrom, V. *J. Am. Chem. Soc.* **2007**, *129*, 8466−8472.
(39) Soci, C.; Hwang, I. W.; Moses, D.; Zhu, Z.; Waller, D.; Gaudiana, R.; Brabec, C. J.; Heeger, A. J. *Adv. Funct. Mater.* **2007**, *17*, 632−636.
(40) Muhlbacher, D.; Scharber, M.; Morana, M.; Zhu, Z. G.; Waller, D.; Gaudiana, R.; Brabec, C. *Adv. Mater.* **2006**, *18*, 2884−2889.
(41) Lin, Y. Z.; Li, Y. F.; Zhan, X. W. *Chem. Soc. Rev.* **2012**, *41*, 4245−4272.
(42) Walker, B.; Kim, C.; Nguyen, T. Q. *Chem. Mater.* **2011**, *23*, 470−482.
(43) Zhu, Z.; Waller, D.; Gaudiana, R.; Morana, M.; Muhlbacher, D.; Scharber, M.; Brabec, C. *Macromolecules* **2007**, *40*, 1981−1986.
(44) Vanelle, P.; Liegeois, C. T.; Meuche, J.; Maldonado, J.; Crozet, M. P. *Heterocycles* **1997**, *45*, 955−962.
(45) Jorgensen, M.; Krebs, F. C. *J. Org. Chem.* **2005**, *70*, 6004−6017.
(46) Wiebeler, C.; Tautz, R.; Feldmann, J.; von Hauff, E.; Da Como, E.; Schumacher, S. *J. Phys. Chem. B* **2013**, DOI: 10.1021/jp3084869.
(47) Polli, D.; Luer, L.; Cerullo, G. *Rev. Scien. Instrum.* **2007**, *78*, 103108.
(48) Frisch, M. J.; Trucks, G. W.; Scuseria, G. E.; Robb, M. A.; Cheeseman, J. R.; Scalmani, G.; Barone, V.; Mennucci, B.; Petersson, G. A.; Nakatsuji, H.; Caricato, M.; Li, X.; Hratchian, H. P.; Izmaylov, A. F.; Bloino, J.; Zheng, G.; Sonnenberg, J. L.; Hada, M.; Ehara, M.; Toyota, K.; Fukuda, R.; Hasegawa, J.; Ishida, M.; Nakajima, T.; Honda, Y.; Kitao, O.; Nakai, H.; Vreven, T.; Montgomery, J. A., Jr.; Peralta, J. E.; Ogliaro, F.; Bearpark, M.; Heyd, J. J.; Brothers, E.; Kudin, K. N.; Staroverov, V. N.; Kobayashi, R.; Normand, J.; Raghavachari, K.; Rendell, A.; Burant, J. C.; Iyengar, S. S.; Tomasi, J.; Cossi, M.; Rega, N.; Millam, J. M.; Klene, M.; Knox, J. E.; Cross, J. B.; Bakken, V.; Adamo, C.; Jaramillo, J.; Gomperts, R.; Stratmann, R. E.; Yazyev, O.; Austin, A. J.; Cammi, R.; Pomelli, C.; Ochterski, J. W.; Martin, R. L.; Morokuma, K.; Zakrzewski, V. G.; Voth, G. A.; Salvador, P.; Dannenberg, J. J.; Dapprich, S.; Daniels, A. D.; Farkas, Ö.; Foresman, J. B.; Ortiz, J. V.; Cioslowski, J.; Fox, D. J. *Gaussian 09*, revision B.01; Gaussian, Inc.: Wallingford, CT, 2009.
(49) Dennington, R.; Keith, T.; Millam, J. *GaussView*, Semichem Inc.: Shawnee Mission KS, 2009.
(50) Zaikowski, L.; Kaur, P.; Gelfond, C.; Selvaggio, E.; Asaoka, S.; Wu, Q.; Chen, H. C.; Takeda, N.; Cook, A. R.; Yang, A.; Rosanelli, J.; Miller, J. R. *J. Am. Chem. Soc.* **2012**, *134*, 10852−10863.
(51) Fazzi, D.; Grancini, G.; Maiuri, M.; Brida, D.; Cerullo, G.; Lanzani, G. *Phys. Chem. Chem. Phys.* **2012**, *14*, 6367−6374.
(52) Kohler, A.; dos Santos, D. A.; Beljonne, D.; Shuai, Z.; Bredas, J. L.; Holmes, A. B.; Kraus, A.; Mullen, K.; Friend, R. H. *Nature* **1998**, *392*, 903−906.
(53) Di Nuzzo, D.; Aguirre, A.; Shahid, M.; Gevaerts, V. S.; Meskers, S. C. J.; Janssen, R. A. J. *Adv. Mater.* **2010**, *22*, 4321.
(54) Siebbeles, L. D. A. *Nat. Chem.* **2010**, *2*, 608−609.
(55) Wilson, M. W. B.; Rao, A.; Clark, J.; Kumar, R. S. S.; Brida, D.; Cerullo, G.; Friend, R. H. *J. Am. Chem. Soc.* **2011**, *133*, 11830−11833.
(56) Chan, W. L.; Ligges, M.; Jailaubekov, A.; Kaake, L.; Miaja-Avila, L.; Zhu, X. Y. *Science* **2011**, *334*, 1541−1545.
(57) Gabor, N. M.; Zhong, Z. H.; Bosnick, K.; Park, J.; McEuen, P. L. *Science* **2009**, *325*, 1367−1371.
(58) Bange, S.; Scherf, U.; Lupton, J. M. *J. Am. Chem. Soc.* **2012**, *134*, 1946−1949.
(59) Lanzani, G. *The Photophysics behind Photovoltaics and Photonics*, 1st. ed.; Wiley-VCH: Weinheim, 2012.
(60) Sreearunothai, P.; Morteani, A. C.; Avilov, I.; Cornil, J.; Beljonne, D.; Friend, R. H.; Phillips, R. T.; Silva, C.; Herz, L. M. *Phys. Rev. Lett.* **2006**, *96*.
(61) Gu, Y.; Wang, C.; Russell, T. P. *Adv. Energy Mater.* **2012**, *2*, 683−690.